ADAPTATION IN CONES

A General Model

STEVAN M. DAWIS AND RICHARD L. PURPLE
Department of Physiology, University of Minnesota, Minneapolis, Minnesota 55455

ABSTRACT Three features appear to characterize steady-state light adaptation in vertebrate cone photoreceptors: (*a*) the shape of the "log intensity–response" curve at different levels of adaptation is the same, the only change with adaptation is in the position of the point on the curve about which the cones operate; (*b*) at high adapting intensities the operating point becomes fixed in position; (*c*) this fixed position is at the steepest point of the log intensity–response curve. These three features can be described by a mathematical model.

INTRODUCTION

It is generally agreed that the first stage of visual adaptation is at the photoreceptor. Under dark-adapted conditions, the peak response of cone photoreceptors grows with increasing stimulus intensity until it saturates (that is, until it reaches a maximal amplitude). Yet under light-adapted conditions, cones continue to transmit information effectively at intensities much higher than that at which the dark-adapted response saturates. Common features have been recognized in the light-adapted behavior of cones in different species. In this paper, a model is presented that incorporates three of these features.

A protocol commonly used to study light adaptation is the steady-state adaptation paradigm. Under this paradigm, the cone system is steadily adapted to an intensity I_a, and a stimulus is applied by suddenly changing the intensity to a new level I_s. The responses evoked by different combinations of I_a and I_s are recorded. Such a set of responses is shown in Fig. 1. These late receptor potentials were obtained, using methods (15, 16) modified by Dawis and Purple (9), from the highly cone-dominated eye of the 13-lined ground squirrel (*Spermophilus tridecemlineatus*). The responses in Fig. 1 have time courses similar to those of macaque cone responses isolated by the foveal local electroretinogram (3, 4). Spectral sensitivity measurements indicated that the ground squirrel late receptor potential reflects mainly green cone activity (Raisanen and Dawis, manuscript in preparation).

A usual data-reduction procedure is to measure the amplitude of the peak change $\hat{R}(I_s|I_a)$ in the response evoked when the intensity is changed from I_a to I_s. [The notation $\hat{R}(I_s|I_a)$ is more economical than the notation $\hat{R}(I_t|I_a)$ used by Dawis (5–7). I_t, I_a, and I_s are related by $I_t + I_a = I_s$.] In Fig. 2 *A*, the peak amplitudes of the responses in Fig. 1 are plotted as a function of $\log(I_s)$. The dark-adapted response function is plotted with filled circles and the two light-adapted response functions with open symbols.

A DESCRIPTION

An accepted description (2, 23) of the dark-adapted response function is the saturating power function

$$\hat{R}(I_s|0) = I_s^n \hat{R}_{max}/(I_s^n + K_r^n) \quad (1)$$

where $\hat{R}_{max}$ is the maximal dark-adapted response, n is an exponent typically between 0.5 and 1.0, and K_r is the familiar semi-saturation constant. [In the notation of Naka and Rushton (23) the semi-saturation constant is given by σ. In the notation of Boynton and Whitten (2) the semi-saturation constant, K_r, is introduced with a typographical error but subsequently presented in correct form by Baron and Boynton (1).] In Fig. 2 *A*, the response amplitudes and stimulus intensities are normalized by $\hat{R}_{max}$ and K_r, respectively.

We tentatively accept the description of the light-adapted cone response functions given in Fig. 2 *B*. The response functions (solid curves) exhibit three important features, first identified by Normann and Werblin (27):

(*a*) The response functions are shape-invariant on an R vs. $\log(I_s)$ plot, the effect of light adaptation being to translate the response function horizontally and vertically. This behavior is displayed by cone response functions of the ground squirrel, as shown in Fig. 2 *A*, and the mudpuppy (27), turtle (25, 26), and macaque (1, 2), as shown in Fig. 3.

(*b*) At high adapting intensities the operating point is fixed. (The operating point is the point on the response function where it intersects the abscissa; this occurs when $I_s = I_a$.) Alternatively, it could be stated that at high adapting intensities Weber's law is obeyed (see Appendix A). Weber's law is obeyed by cone responses in the macaque (2), frog (11, 20), carp (29), mudpuppy (27), turtle (25), and walleye (D. Burkhardt, personal communication).

(*c*) At high adapting intensities the operating point is at the steepest point of the response function. This ensures an optimal sensitivity at high adapting intensities. As will be seen, many cone systems possess this feature.

A MODEL

A model that exhibits feature *a* is

$$\hat{R}(I_s|I_a) = \hat{R}(p(I_a)I_s|0) - \hat{R}(p(I_a)I_a|0) \quad (2)$$

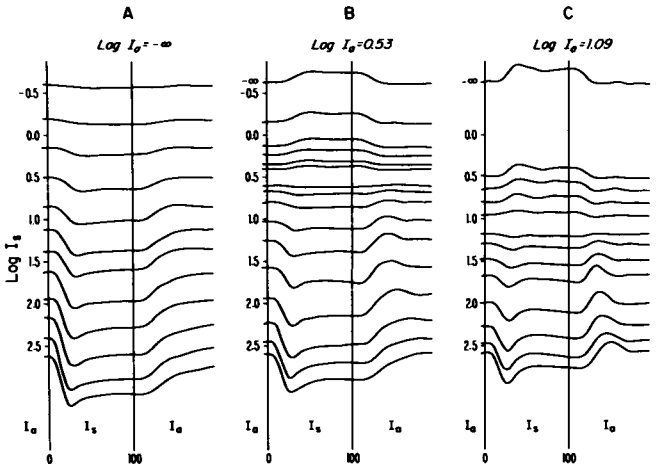

FIGURE 1 Late receptor potentials isolated in the 13-lined ground squirrel eye by injection of a single 1.5 ml bolus of 100 mM sodium L-aspartate solution into the vitreous. Records are computer-averaged responses to step changes in light intensity. White light (color temperature ~5,100°K) was used for stimulation and adaptation. The stimulus duration was 100 ms; interstimulus period was 5–10 s long. (*A*) A dark-adapted intensity series obtained 40 min after aspartate injection. During the 40 min, the eye was adapted to darkness. (*B* and *C*) Two light-adapted intensity series. In each case, 20 min was allowed for light adaptation.

where $p(I_a)$ is a decreasing function of I_a and has values ranging from 1 to 0. Note that Eq. 2 tells us how to construct light-adapted response functions, $\hat{R}(I_s|I_a)$, from the dark-adapted response function, $\hat{R}(I|0)$, provided that $p(I_a)$ is known. In words, Eq. 2 states that the peak change $\hat{R}(I_s|I_a)$ in the response evoked when a stimulus intensity I_s suddenly replaces a steady-adapting intensity I_a can be calculated as follows: First, take the stimulus intensity I_s and the adapting intensity I_a and attenuate them by the factor $p(I_a)$; this computation results in an attenuated stimulus intensity of $p(I_a)I_s$ and an attenuated adapting intensity of $p(I_a)I_a$. Second, calculate the amplitudes of the responses that these attenuated intensities would give in the dark. This calculation is done by substituting the attenuated intensities into the dark-adapted response function $\hat{R}(I|0)$. Hence, if the attenuated stimulus intensity were presented in the dark, it would cause a peak change in response of amplitude $\hat{R}(p(I_a)I_s|0)$, and if the attenuated adapting intensity were presented in the dark, it would cause a peak change in response of amplitude $\hat{R}(p(I_a)I_a|0)$. Finally, to compute $\hat{R}(I_s|I_a)$ take the difference of the calculated response amplitudes $\hat{R}(p(I_a)I_s|0)$ and $\hat{R}(p(I_a)I_a|0)$. Thus, the strategy to prevent the system from saturating is to attenuate incoming light by a factor that depends on the intensity of the adapting light. We have found that a good empirical description of p is given by

$$p(I_a) = K_d/(I_a + K_d) \quad (3)$$

where K_d is a positive-valued constant. Note that there is no attenuation of incoming light when the system is dark adapted [that is, $p(I_a) = 1$ when $I_a = 0$] and that incoming light becomes more attenuated as the system adapts to more intense lights [that is, $p(I_a) \to 0$ as $I_a \to \infty$]. The function in Eq. 3 can be generated by mechanisms described by Dawis (5). The model given by Eqs. 1–3 will exhibit features *b* and *c*, as well as *a*, provided that

$$K_d = K_r \quad (4)$$

(see Appendix B for a proof).

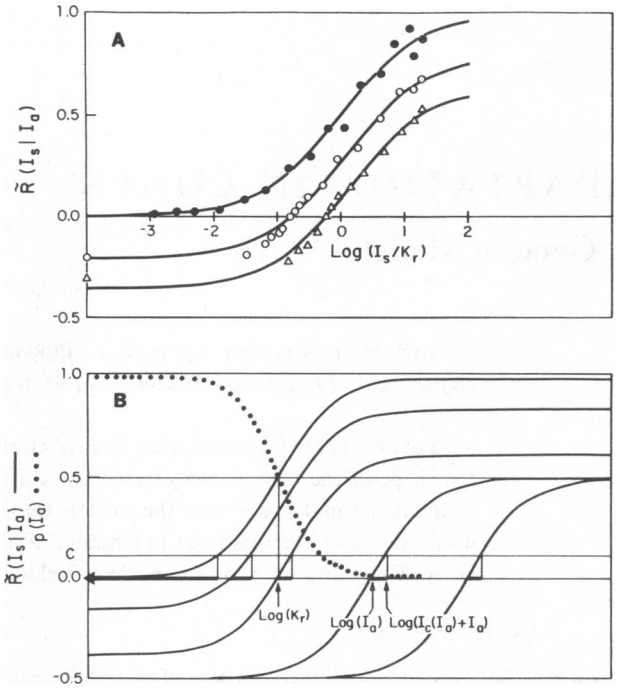

FIGURE 2 (*A*) Normalized peak response amplitudes, $\tilde{R}$, plotted as a function of normalized log stimulus intensity, $\log(I_s/K_r)$. ●, dark-adapted data in Fig. 1 *A*; ○, light-adapted data in Fig. 1 *B*, and △, light-adapted data in Fig. 1 *C*. (*B*) An illustration of three features of cone steady-state adaptation. The graph is actually two superimposed plots: solid lines, an $\tilde{R} - \log(I_a)$ plot and dotted lines, a $p - \log(I_a)$ plot. The solid lines are five response functions generated by Eqs. 1–4 with $n = 0.7$ and $\tilde{R}_{max} = 1.0$. The response functions correspond to adapting intensities of $\log(I_a/K_r) = -\infty$, -1, 0, 2, and 4. The dotted line represents an attenuating function generated by Eqs. 3 and 4. Boynton and Whitten (2) have suggested that a plot of the steady-state fraction of unbleached photopigment would superimpose on the dotted curve (compare with Fig. 2 of reference 2).

DISCUSSION

Surprisingly, when Eqs. 1–3 are fitted to the available cone adaptation data, the fourth relationship, Eq. 4, emerges. The "least-squares error" fit by Eqs. 1–3 to the ground squirrel data is shown by the solid curves in Fig. 2 *A*. The corresponding values for n, K_r, and K_d are listed in Table I. Because of limitations in our work (viz. it was impossible with our apparatus to provide enough stimulus intensity to saturate the ground squirrel late receptor potential), we tested the model against published electrophysiological data obtained from the mudpuppy (27), turtle (25), and macaque (1, 2). The results of this analysis are shown in Fig. 3, and the best-fitting parameter values are listed in Table I. For each system, $K_d \sim K_r$.

The model, Eqs. 1–4, is also consistent with human psychophysical data. Corresponding to the shape-invariance of cone response functions is the shape-invariance of cone increment threshold functions observed psychophysically by Geisler (14). Values for K_r and K_d can be extracted from Fig. 8 *a* of Geisler (14) since, on a $\log[K_r/p(I_a)] - \log(I_a)$ plot, the model predicts asymptotic slopes

TABLE I
PARAMETRIC VALUES FOR CONE STEADY-STATE ADAPTATION*

Investigators (species)	n	K_r	K_d	K_{pb}
Boynton and Whitten (2) (*Macaca irus*)	0.503	95,100 trolands	7,600 tds	10,000 tds
Baron and Boynton (1) (*Macaca irus*)	0.462	7,760 trolands	295 tds	10,000 tds
Normann and Werblin (27) (*Necturus maculosus*)	0.677	19,700 units	16,000 units	$>2 \times 10^7$ units
Normann and Perlman (25) (*Pseudemys scripta elegans*)	0.850	454 units	515 units	?
Dawis and Purple (Fig. 2*A*) (*Spermophilus tridecemlineatus*)	0.697	1.00 units	1.53 units	?
Geisler (14) (human)	0.7	166 trolands	194 tds	15,800 tds

*In all cases, with the exception of the human psychophysical measurements, values given for n, K_r, and K_d are those of the dark-glasses model that best fits (least-squares error) the data.

of 0 and 1 intersecting at $[\log(K_d), \log(K_r)]$. The result is listed in Table I, and once again $K_d \sim K_r$.

The model (and the three features) may also describe adaptation in the photoreceptor responses of the blowfly and dragonfly (see Fig. 3 of reference 21) and in the growth rate of phycomyces (see Fig. 7 of reference 10).

The proposed model is closely related to earlier models of adaptation. Eq. 1, used to describe dark-adapted responses, is the empirical model of Naka and Rushton (23) as modified by Boynton and Whitten (2). To describe light-adapted responses, Naka and Rushton (24) suggested the model $\hat{R}(I_s|I_a) = \hat{R}(I_s|0) - \hat{R}(I_a|0)$. Since this model can not reproduce Weber's law (5, 8, 17, 18, 28), it is inadequate in describing cone light-adapted behavior.

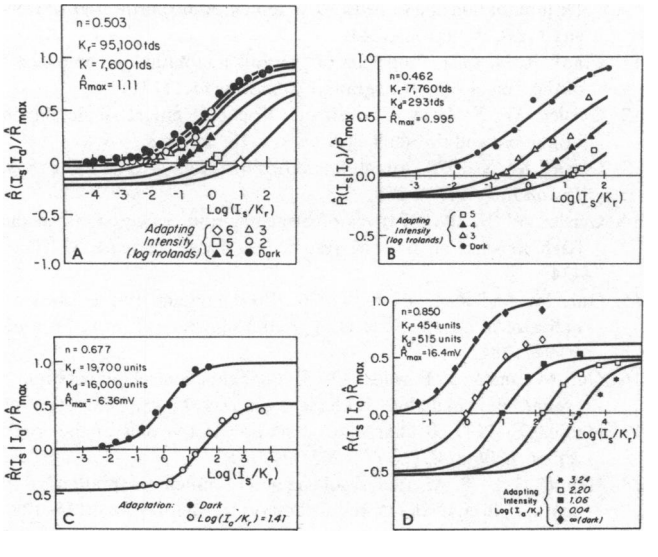

FIGURE 3 Response function data fitted (least-squares error) by Eqs. 1–3. *A*, data of Boynton and Whitten (2) from the macaque; *B*, data of Baron and Boynton (1) from the macaque; *C*, data of Normann and Werblin (27) from the mudpuppy; *D*, data of Normann and Perlman (25) from the turtle.

Eq. 2 is very similar to Naka and Rushton's (24) model for light adaptation, the important difference is that in Eq. 2 the intensities I_s and I_a are attenuated by a factor $p(I_a)$. Normann and Werblin (27) suggested that light adaptation in cones has an effect equivalent to placing a neutral density filter in the light beam. MacLeod (22) referred to models of this kind as "dark glasses" models. Eq. 2 is a dark glasses model. The model formed by combining Eqs. 1 and 2 has recently attracted attention. A simple algebraic manipulation reveals that this model belongs to the class of models in which the apparent σ is dependent on I_a (25). For Eqs. 1 and 2, $\sigma(I_a) = K_r/p(I_a)$. Similar variable σ models have been suggested by Hood et al. (19) and Geisler (14) to describe cone saturation increment threshold functions. In fact, Geisler's (12–14) approach and ours is in agreement (Chap. 10 of reference 7). Finally, consider the model given by Eqs. 1–3 with

$$K_d = K_{pb} \tag{5}$$

where K_{pb} is the half-bleaching constant of the cone photopigment. This model, Eqs. 1–3, and 5, is the Boynton-Whitten (2) model. For the Boynton-Whitten model, $p(I_a)$ is the fraction of cone photopigment left unbleached by the steady-adapting light. In their eleventh footnote (which contains a serious typographical error), Boynton and Whitten (2) noted that the relationship

$$K_{pb} = K_r \tag{6}$$

seemed to obtain. Boynton and Whitten (2) were "uncertain whether this agreement [was] fortuitous, or of theoretical significance." Since Eq. 6 can be obtained by combining Eqs. 4 and 5 its significance is revealed: for the Boynton-Whitten model, equality of K_{pb} and K_r ensures that at high adapting intensities the operating point is at the steepest point of the response function. In Table I, K_{pb} values measured or estimated by the respective authors are

given. According to the Table, Eqs. 5 and 6 do not hold for the mudpuppy and human cones and the case for macaque cones is equivocal. Presently, only the proposed model, Eqs. 1–4, gives a general description of cone adaptation.

APPENDIX A

A result of fixing the high intensity operating point is that

$$I_C(I_a) = k \cdot I_a \text{ for large } I_a, \quad (7)$$

where $I_C(I_a)$ is the intensity increment needed on I_a to produce a response of criterion amplitude and k is a positive-valued constant. (Eq. 7 is a neural analogue to Weber's law of psychophysics.)

Proof

Normann and Werblin (27) proved that if over a range of adapting intensities the response functions on an $\hat{R}-\log(I_a)$ plot intersect the abscissa with the same slope, then Weber's law is obeyed over that range of intensities. In Fig. 2 *B* the two right-most response functions intersect the abscissa with the sample slope; at these high adapting intensities Weber's law is obeyed.

Although Normann and Werblin's proof applies only when the criterion amplitude is infinitesimally small, it is an easy matter to generalize to criteria of finite magnitude: If over a range of adapting intensities the response functions on an $\hat{R}-\log(I_a)$ plot are (*a*) shape-invariant and (*b*) have a fixed operating point, then Weber's law is obeyed over that range of intensities. To prove this last claim, let us consider the case shown in Fig. 2 *B*. In this figure, a hypothetical criterion level C is shown. The thick bars on the $\log(I_a)-$axis indicate the distance, for each response function, from $\log[I_C(I_a)+I_a]$ to $\log(I_a)$. At high intensities, where the operating point is fixed, this length is constant. Denoting this constant length by $\log(1+k)$, one gets $\log[I_C(I_a)+I_a] - \log(I_a) = \log(1+k)$, which leads to Eq. 7.

APPENDIX B

The model given by Eqs. 1–4 possesses features *a–c*.

Proof

First, the response functions of the model are shape-invariant on an $\hat{R}-\log(I_a)$ plot with light adaptation producing a horizontal translation of $-\log[p(I_a)]$ and a vertical translation of $-\hat{R}(p(I_a)I_a|0)$ (see references 6 and 7). Second, the model obeys Weber's law at high intensities, provided that $(K_r/K_d)^n > C/(1-C)$ where C is the normalized criterion level (see references 5 and 7). Given Eq. 4 this condition becomes $1 > C/(1-C)$, a condition easily satisfied. Third, to see that the model optimizes its sensitivity at high adapting intensities, consider the ratio $[\hat{R}_{max}-\hat{R}(p(I_a)I_a|0)]/\hat{R}(p(I_a)I_a|0)$. For each I_a, this ratio is equal to "the response range available to incremental stimulation" divided by "the response range available to decremental stimulation." For the model given by Eqs. 1–3 this ratio approaches a value of $(K_r/K_d)^n$ as I_a becomes very large. With the addition of Eq. 4 this asymptotic value becomes 1. This means that the complete model, Eqs. 1–4, translates the response function such that at high adapting intensities half the response range is above the abscissa and half the range below. As Fig. 2 *B* illustrates, on an $\hat{R}-\log(I_a)$ plot, the steepest point of a saturating power function is at its mid-point. Therefore, Eq. 4 ensures that at high adapting intensities the model will operate about the steepest point of the response function on an $\hat{R}-\log(I_a)$ plot. [A completely analytical solution gives the same answer; see reference 7. The analytical solution states that if the response functions are shape-invariant on an $\hat{R}-\log(I_a)$ plot, then to get optimal sensitivity at high adapting intensities, the high intensity operating point must correspond to a point on the dark-adapted response function where $d\hat{R}/dI + I \cdot d^2\hat{R}/dI^2 = 0$, in other words, to a point on the dark-adapted response function where it is steepest on an $\hat{R} - \log(I)$ plot.]

We thank Drs. Charles Knox, John Soechting, and John Anderson for supplying various computer programs. We thank Drs. Reichardt and Geisler for bringing their results (references 10 and 14, respectively) to our attention.

This work was supported in part by United States Public Health Service grant EY 00293. Computer facilities were made available by Air Force Office of Scientific Research grants AF-AFOSR(AFSC)–1221, AFOSR 71–1969, and AFOSR 75–2804.

Received for publication 10 September 1980 and in revised form 26 March 1982.

REFERENCES

1. Baron, W. S., and R. M. Boynton. 1974. The primate foveal local electroretinogram: an indicator of photoreceptor activity. *Vision Res.* 14:495–501.
2. Boynton, R. M., and D. N. Whitten. 1970. Visual adaptation in monkey cones: recordings of late receptor potentials. *Science (Wash., D. C.).* 170:1423–1426.
3. Brown, K. T., and K. Watanabe. 1962. Isolation and identification of a receptor potential from the pure cone fovea of the monkey retina. *Nature (Lond.).* 193:958–960.
4. Brown, K. T., K. Watanabe, and M. Murakami. 1965. The early and late receptor potentials of monkey cones and rods. *Cold Spring Harb. Symp. Quant. Biol.* 30:457–482.
5. Dawis, S. M. 1978. A model for light adaptation: producing Weber's law with bleaching-type kinetics. *Biol. Cybern.* 30:187–193.
6. Dawis, S. M. 1979. Light adaptation in cone photoreceptors: the occurrence and significance of unitary adaptive strength. *Biol. Cybern.* 34:35–41.
7. Dawis, S. M. 1980. Steady-State Adaptation in Cone Photoreceptors. Ph.D. thesis. University of Minnesota, Minneapolis, MN 435 pp.
8. Dawis, S. M. 1981. The compression model: a re-examination. *Vision Res.* 21:1511–1515.
9. Dawis, S. M., and R. L. Purple. 1981. Steady-state adaptation in the ground squirrel retina: PIII and b-wave intensity response functions. *Vision Res.* 21:1169–1180.
10. Delbrück, M., and W. Reichardt. 1956. System analysis for the light growth reactions in phycomyces. *In* Cellular Mechanisms in Differentiation and Growth. D. Rudnick, editor, Princeton University Press, Princeton. 3–44.
11. Frank, R. N. 1971. Properties of "neural" adaptation in components of the frog electroretinogram. *Vision Res.* 11:1113–1123.
12. Geisler, W. S. 1978. The effects of photopigment depletion on brightness and threshold. *Vision Res.* 18:269–278.
13. Geisler, W. S. 1978. Adaptation, after images and cone saturation. *Vision Res.* 18:279–289.
14. Geisler, W. S. 1981. Effects of bleaching and backgrounds on the flash response of the cone system. *J. Physiol. (Lond.).* 312:413–434.
15. Gur, M., and R. L. Purple. 1976. Blood pressure responses as an indicator of anesthetic level in ground squirrels. *J. Appl. Physiol.* 40:977–981.
16. Gur, M., and R. L. Purple. 1978. Retinal ganglion cell activity in the ground squirrel under halothane anesthesia. *Vision Res.* 18:1–14
17. Hemilä, S. 1977. Background adaptation in the rods of the frog's retina. *J. Physiol. (Lond.).* 265:721–741.
18. Hemilä, S. 1978. An analysis of rod outer segment adaptation based on a simple equivalent circuit. *Biophys. Struct. Mech.* 4:115–128.
19. Hood, D. C., M. A. Finkelstein, and E. Buckingham. 1979. Psychophysical tests of models of the response function. *Vision Res.* 19:401–406.
20. Hood, D. C., and P. A. Hock. 1975. Light adaptation of the receptors: increment threshold functions for the frog's rods and cones. *Vision Res.* 15:545–553.
21. Laughlin, S. B., and R. C. Hardie. 1978. Common strategies for light

adaptation in the peripheral visual system of the fly and dragonfly. *J. Comp. Physiol.* 128:319–340.

22. MacLeod, D. I. A. 1978. Visual sensitivity. *Annu. Rev. Psych.* 29:613–645.
23. Naka, K. I., and W. A. H. Rushton. 1966. S-potentials from colour units in the retina of the fish (*Cyprinidae*). *J. Physiol.* (*Lond.*). 185:536–555.
24. Naka, K. I., and W. A. H. Rushton. 1966. S-potentials from luminosity units in the retina of the fish (*Cyprinidae*). *J. Physiol.* (*Lond.*). 185:587–599.
25. Normann, R. A., and I. Perlman. 1979. Evaluating sensitivity changing mechanisms in light-adapted photoreceptors. *Vision Res.* 19:391–394.
26. Normann, R. A., and I. Perlman. 1979. The effects of background illumination on the photoresponses of red and green cones. *J. Physiol.* (*Lond.*). 286:491–507.
27. Normann, R. A., and F. S. Werblin. 1974. Control of retinal sensitivity. I. Light and dark adaptation of vertebrate rods and cones. *J. Gen. Physiol.* 63:37–61.
28. Williams, T. I., and J. G. Gale. 1977. A critique of an incremental threshold function. *Vision Res.* 17:881–882.
29. Witkovsky, P., J. Nelson, and H. Ripps. 1973. Action spectra and adaptation properties of carp photoreceptors. *J. Gen. Physiol.* 61:401–423.